

©1991 Society of Photo-Optical Instrumentation Engineers. This paper was published in SPIE Vol. 1584 Fiber Optic and Laser Sensors IX (1991) and is made available as an electronic reprint with permission of SPIE. One print or electronic copy may be made for personal use only. Systematic or multiple reproduction, distribution to multiple locations via electronic or other means, duplication of any material in this paper for a fee or for commercial purposes, or modification of the content of the paper are prohibited.

## A symmetric 3x3 coupler based demodulator for fiber optic interferometric sensors

David A. Brown, Charles B. Cameron, Robert M. Keolian, David L. Gardner, and Steven L. Garrett

Physics Department, Code PH/Gx, Naval Postgraduate School, Monterey, CA 93943

### ABSTRACT

A method for demodulation of fiber optic interferometric sensors that utilizes a 3 x 3 coupler is described. The passive demodulation scheme does not require carrier (phase) modulation. The demodulation scheme relies on the three outputs of a 3 x 3 coupler and uses all three of its phase modulated output signals to recreate the stimulus inducing the original optical phase modulation. The demodulator scale factor (volts/radian) is stable against fluctuations in both fringe visibility and average received power. Upon initial implementation of the scheme, a dynamic range of 116 dB was obtained (at 600 Hz in a 1 Hz bandwidth with maximum THD at 4%). The minimum detectable signal at 600 Hz was  $220 \mu\text{rad}/\sqrt{\text{Hz}}$  and the maximum tolerable signal was 140 radians. Both the maximum tolerable signal and the minimum detectable signal (noise floor) was observed to increase with decreasing frequency. Thus, depending on the frequency, the demodulation scheme is capable of detecting phase signals less than a milliradian to in excess of kiloradians.

### 1. INTRODUCTION

Since the first application of optical fiber interferometry as a means of detecting acoustical signals [Ref 1], there has been a steady series of improvements to the sensitivity and selectivity of the transducer, the noise characteristics of laser sources, and the detectability limits of demodulator circuitry. In regard to demodulation schemes for phase modulated (interferometric) sensors, by far the most common techniques rely on some form of carrier (phase) modulation in order to demodulate the phase encoded signals that are interferometrically converted into intensity modulations with a 2x2 coupler. The intrinsic problem with 2x2 couplers is due to energy conservation, which causes the outputs to be  $180^\circ$  out-of-phase. When one of the 2 x 2 outputs is at its maximum, the other must be a minimum, since the total optical power out of the coupler, which is a passive device, must be constant for a constant input power. Thus, there are certain phases (0,  $180^\circ$ , etc.) where the change of output with respect to phase is zero. Therefore, external modulation is often introduced to account for this problem by making available both in-phase and quadrature information. In the phase generated carrier demodulator, the phase modulated signal is typically recovered using heterodyne techniques and a sine-cosine demodulation process.

One example is a pseudo-heterodyne demodulation system which produces a phase generated carrier [Ref. 2] by modulating the wavelength of the laser diode. Wavelength modulation in the interferometer is typically achieved by modulating the current to the laser diode light source which, in addition to producing an unwanted modulation of the light intensity, results in a thermally induced change in the index of refraction and length of the laser cavity. It is more direct to insert a piezoelectric modulator in one of the legs of the interferometer in order to achieve a carrier modulation. However, this violates the motivation and advantages inherent in using fiber optic sensors. In order to produce a net phase modulation, the interferometer must be unbalanced by including an optical path difference (OPD) between the legs of the interferometer, since an interferometer is intrinsically a differential device. The magnitude of the laser current induced phase modulation scales linearly with the OPD in the interferometer. However, the phase noise in the interferometer due to frequency jitter in the interferometer also increases linearly with OPD.

Researchers using this phase generated carrier demodulation approach are well aquatinted with its many problems, which include: 1) the requirement for expensive stable diodes having long coherence lengths, 2) noisy operation due to mode hopping often induced from the superimposed current

modulation, 3) high setup complexity requiring FFT calibration of phase generated carrier spectral components to insure Bessel function balance and orthogonality, 4) the necessity of an OPD which introduces additional laser noise and uncompensated environmental induced signals, 5) fluctuations in sensor output due to scale factor instability, (scale factor quantifies the circuit's conversion of optical phase in radians to electrical output in volts), and 6) the signal of interest appears as sidebands at the carrier frequency and at its harmonics.

In an ideal, equal split ratio, 3 x 3 coupler, the outputs have a relative phase difference of 120° which allows one to generate the in-phase and quadrature signals without the carrier waveform. In previous research using 3x3 based demodulators [Ref. 3], only two of the three available outputs from the 3 x 3 coupler were used in recreating the in-phase and quadrature signals and these signals were again processed by the sine-cosine demodulation algorithm used for the phase generated carrier technique. Although, this approach does alleviate many of the problems associated with phase generated carrier demodulation, such as light source wavelength modulation, the optical path mismatch, and Bessel function balance and orthogonality, the unavailability of stable 3x3 couplers postponed the practical implementation of this strategy. Recently, 3 x 3 couplers with good environmental stability and polarization insensitivity have become available [Ref. 4] and are offered by a number of commercial coupler manufacturers.

## 2. ADVANTAGES OF SYMMETRIC 3X3 COUPLER BASED DEMODULATION

In the present algorithm, all three outputs of the 3x3 coupler are used in a symmetric manner to recreate the phase modulated signal. No modulation of the light source wavelength is required. This reduces noise and cost since there is less probability that the laser will "mode hop". The current induced frequency modulation characteristic, or dv/di parameter, is not a consideration in choosing the laser. No optical path difference is required in the legs of the interferometer. This insures that laser phase noise is substantially reduced. This also implies that the coherence length of the laser used as the light source can be significantly shorter than that otherwise, and hence less expensive laser diodes can be used. Since the signals required for demodulation are not extracted as sidebands of a carrier, no Bessel amplitude equalization or orthogonalization is required. The new symmetric demodulation technique is capable of demodulating signals of amplitude in the hundreds of radians level whereas the phase generated carrier technique is typically limited to maximum signals on the order of a radian. This feature has the advantage of allowing exploitation of newly developed, high sensitivity, push-pull and air-backed fiber optic interferometric transducers that produce signals which are 20 to 50 dB greater than previous topologies [Ref. 5-9]. Possibly, the most important characteristic of this style demodulator is that it uses a simple automatic gain control circuit that is capable of maintaining a stable scale factor (volts/radian) in the presence of variations in the total power and in the fringe visibility.

## 3. SYMMETRIC DEMODULATION DESCRIPTION AND OPERATION

A Mach-Zehnder fiber optic interferometer consisting of a 2x2 coupler at the input and a 3x3 coupler at the output was fabricated in order to test the symmetric demodulation algorithm [Ref. 10-11]. Each leg of the interferometer was wrapped around a separate piezoelectric cylinder as shown in the schematic diagram in Figure 1. The piezo-cylinders were driven 180° out-of-phase so as to produce large modulation amplitudes in the interferometer.

The power from each leg of the 3x3 coupler is nominally 120° out of phase with either of its neighbors and can be expressed as

$$x_n = C + B \cos \left[ \phi(t) - (n-1) \frac{2}{3} \pi \right], \quad (1)$$

where  $n$  is a labeling index having value 1, 2, or 3,  $\phi(t)$  is the phase modulation between the legs of the interferometer, and  $C$  is a central value around which the output will vary with amplitude  $B$ ,

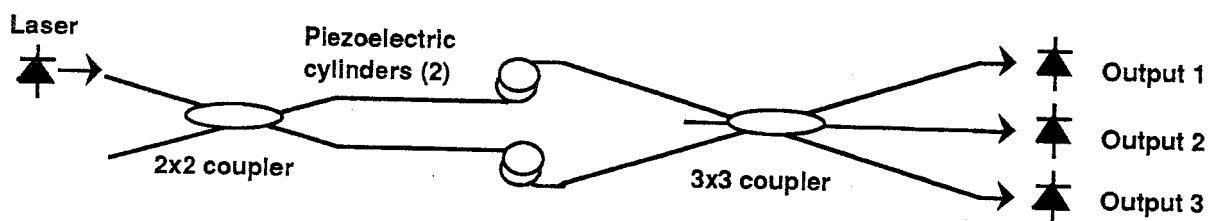


**Figure 1.** Schematic diagram of a Mach-Zehnder interferometer terminated with a 3x3 coupler. Each of the two interferometer legs were wrapped on piezoelectric cylinders in order to generate phase modulations to verify the performance of the 3x3 symmetric demodulation scheme.

For illustrative purposes let us examine the resulting waveform described by equation 1 due to a monofrequency excitation (in this case a voltage applied differentially to the piezoelectric cylinders) that produces a phase modulation of amplitude  $5\pi$  radians, i.e.,  $\phi(t) = 5\pi \sin(2\pi ft)$ . The resulting intensity modulation from the legs of the interferometer is simulated in Figure 2. Note that the waveforms are  $120^\circ$  out-of-phase, the three simulated outputs have been normalized and shifted relative to one another and the superimposed monofrequency stimulus is also shown. These waveforms are obviously not proportional to the applied stimulus; thus one would expect a nonlinear circuit will be needed to reconstruct the original stimulus. Although this may seem to be a disadvantage for using interferometric sensors, there are certain applications where this non-linear feature might be attractive. For example, cases may exist where large low frequency signals are present, which would otherwise produce an output in linear systems that could saturate the detection electronics. Although, the phase modulated waveform bears little resemblance to the original stimulus, there are features that do correlate, such as the periodicity of the waveforms, and the symmetry that exists between the amplitude and slope of the stimulus waveform with the resulting frequency content of the interferometric waveform. In the simple example of interferometric phase modulation arising from a single frequency, it is that sine wave which we hope to recover. Although, the demodulation scheme does work equally well with multifrequency waveforms or noise. In Figure 3, we present a block diagram describing the technique of symmetric demodulation using the three outputs from a 3x3 coupler

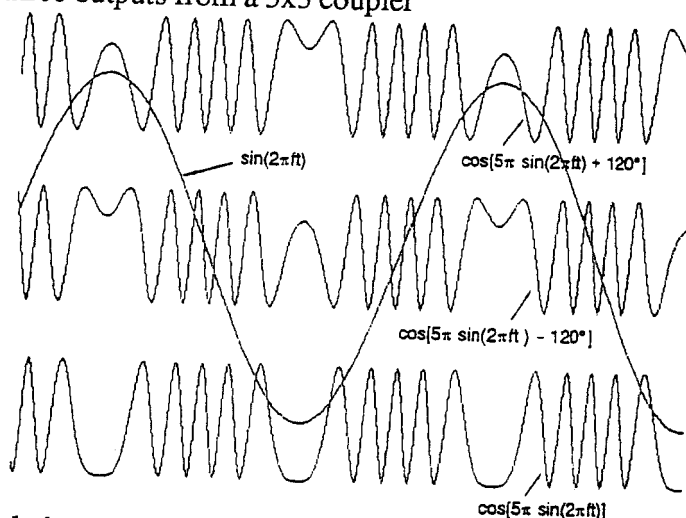


**Figure 2.** A simulated phase modulated signal of amplitude  $5\pi$  radians. Three of the waveforms represent the outputs from a 3x3 coupler. The superimposed sine wave is proportional to phase modulation induced between the legs of the interferometer.

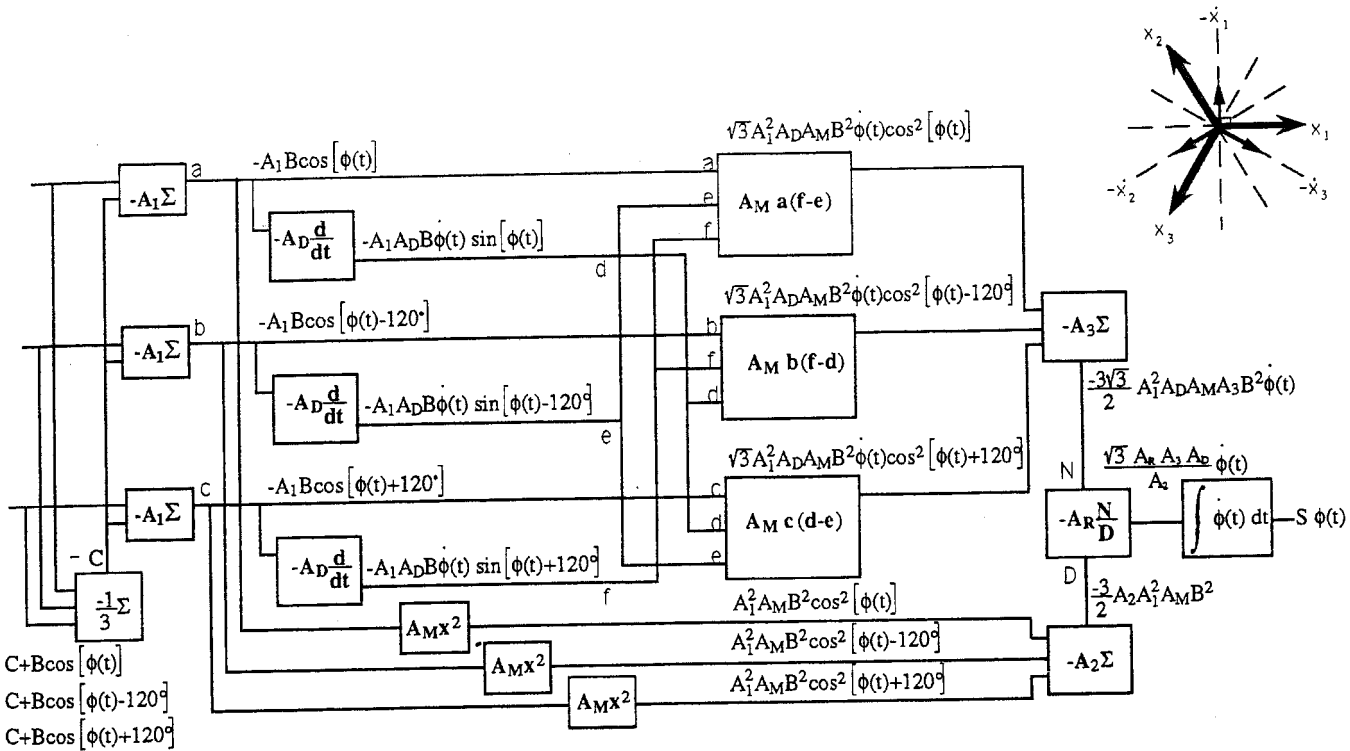


**Figure 3.** Block diagram of the symmetric demodulator and a phasor representation of the signals and their derivatives (upper right of the figure).

As an alternative to low pass filtering the signal from the photodetector to remove the DC offset thereby compromising the ability to demodulate low frequency and sub-fringe phase modulations due to the DC contents of these signals, we subtract "C" from each of the inputs to the demodulator circuit, thereby preserving the low frequency content of the signal. The DC offset, "C", is obtained by adding the three inputs and choosing the gain of the adder to be  $-1/3$ . The cosine terms cancel as a result of this addition, by the trigonometric identity

$$\sum_{n=1}^3 \cos \left[ \xi - (n-1) \frac{2\pi}{3} \right] = 0 \quad (2)$$

After subtracting "C" from each signal, we take the derivative of each and arrive at

$$-A_1 A_D B \dot{\phi}(t) \sin[\phi(t) - (n-1)2\pi/3] \quad (3)$$

where  $A_1$  is the gain of the adder and  $A_D$  is the gain of the differentiator. Each signal with is multiplied by the difference of the derivatives of the two remaining signals, so that the output of the multiplier is a cosine squared function of the form,

$$(\sqrt{3} A_D A_M A_I^2) B^2 \dot{\phi}(t) \cos^2 \left[ \phi(t) - (n-1)\frac{2\pi}{3} \right], \quad (4)$$

whose amplitude is proportional to the derivative of the phase modulation. This result arises from the trigonometric identity  $\sin(\alpha + \beta) - \sin(\alpha - \beta) = 2\cos(\alpha)\sin(\beta)$ , which has been applied to the difference of the two derivatives with  $\alpha = \phi(t)$  and  $\beta = 2\pi/3$ . Next, the three similar outputs are summed to remove the cosine squared dependence on  $\phi(t)$ . The output of the summer having gain  $A_3$ , is

$$\left( \frac{3\sqrt{3}}{2} A_D A_M A_I^2 A_3 \right) B^2 \dot{\phi}(t). \quad (5)$$

Equation 5 makes use of the trigonometric identity,

$$\sum_{n=1}^N \cos^2 \left[ \xi - (n-1)\frac{2\pi}{3} \right] = \frac{N}{2}, \quad (6)$$

which is a generalization of the more familiar expression  $\sin^2\xi + \cos^2\xi = 1$ , for  $N > 2$ . To remove the  $B^2$  dependence in equation 5, we employ a simple automatic gain control circuitry (AGC) consisting of an analog divider chip whose numerator is that of equation 5, and whose denominator is obtained by taking the sum of the squares of the three input signals (with "C" removed). Thus again invoking the identity of equation 6, we divided equation 5 by the quantity

$$\left( \frac{3}{2} A_M A_I^2 A_2 \right) B^2 \quad (7)$$

where  $A_M$  is the gain in the squaring circuit and  $A_2$  is the gain of the summer circuit. Thus the output of the AGC, having gain  $A_R$ , becomes independent of the AC power in the interferometric signal. Prior to integration the signal is of the form:

$$\frac{\sqrt{3} A_3 A_D A_R}{A_2} \dot{\phi}(t). \quad (8)$$

The signal is then integrated and we arrive at a signal proportional to  $\phi(t)$ , the original phase modulation, with, of course, an additional gain factor,  $A_I$ , due to the integrator. Hence, the voltage-to-phase demodulation scale factor,  $S$ , can be expressed as,

$$S = \frac{v(t)}{\phi(t)} = \frac{\sqrt{3} A_I A_3 A_D A_R}{A_2}. \quad (9)$$

## 4. SYMMETRIC DEMODULATOR PERFORMANCE

### 4.1 Scale Factor Stability

The symmetric demodulator scale factor stability is illustrated in Figure 4. Typical phase generated carrier demodulation techniques have a one-to-one correspondence in the change in AC power and scale factor. This is very important, since, in principle, there is no way to distinguish fluctuations in scale factor from real signals. Thus scale factor stability is important for practical fiber optic sensing systems. The diode laser used in this experiment was a Sharp 830nm, type LT015 that was pigtailed (by Seastar Optics) with a 125 $\mu$ m cladded single mode optical fiber.

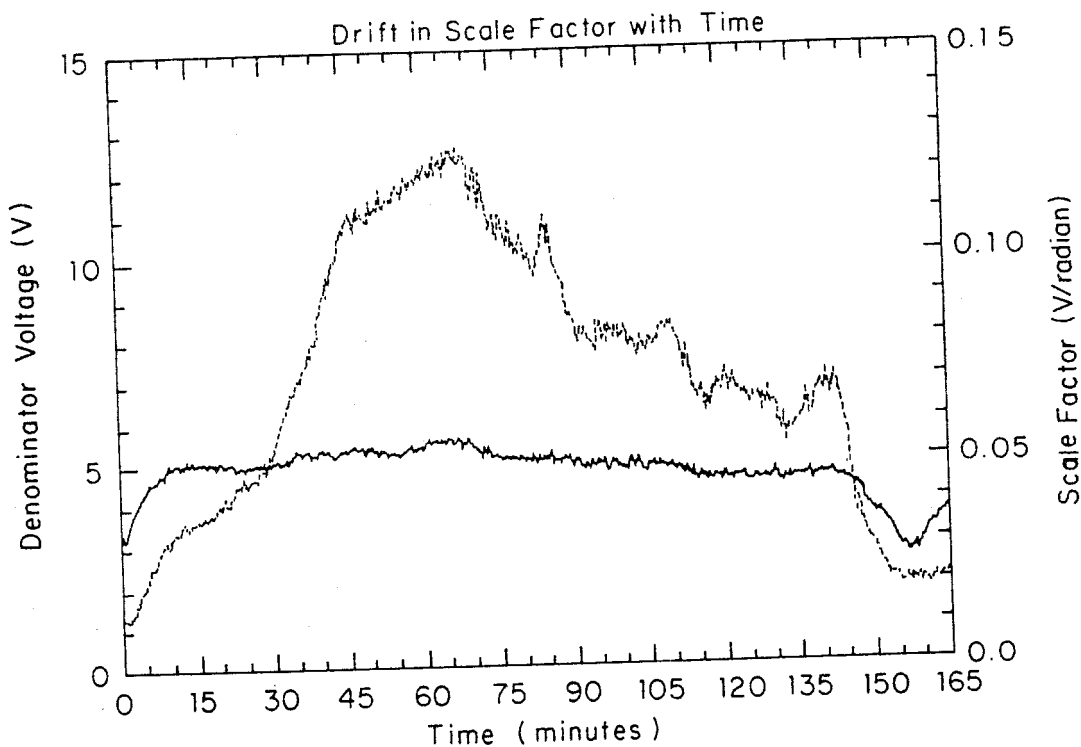


**Figure 4.** Scale factor drift for the symmetric demodulator over 165 minutes of operation. The dashed trace is proportional to the square of the AC portion of the optical power received by the demodulator circuit (left vertical axis labeled "Denominator Voltage"). The solid trace is the Scale Factor for the symmetric demodulator (right vertical axis). When the denominator voltage exceeds 4 Volts, the scale factor is seen to be stable to better than  $\pm 5\%$  even in the presence of variations that are greater than a factor of three in the square of the AC portion of the optical power.

## 2 Dynamic Range

The dynamic range of the demodulator is defined as the ratio of the maximum signal that can be accurately reproduce by the circuit to the minimum detectable signal in a given bandwidth. A conservative criteria defining the maximum signal was chosen as that amplitude for which the demodulated output exceeded a total harmonic distortion level (THD) of 4%. For the detectability, the bandwidth of the measurement has been normalized to 1 Hertz. The dynamic range in a 1 Hz bandwidth at 4% THD is thus displayed in Figure 5. The plateau in dynamic range at low frequencies is an artifact of the inability to generate sufficient modulation levels at low frequencies in the piezoelectric cylinders. Thus a projected performance dotted-line has been superimposed of the plot. The minimum detectable signal at 600 Hz is  $220 \mu\text{rad}/\sqrt{\text{Hz}}$  and the maximum tolerable signal level is 140 radians, thus the dynamic range is 116 dB.

From Figure 5, it is seen that the maximum and minimum signal levels are proportional to "1/f" (-20 dB/decade). For the maximum signal, this is due to the maximum fringe rate of the demodulator (65 krad/sec). The 1/f dependance in the detectability was due to integration of the multiplier noise. This performance leads to a constant dynamic range for the system, which is well suited for practical use, since, laser noise, ocean noise, and many other systems exhibit this well known (but still unexplained) characteristic "flicker" noise at low frequencies.

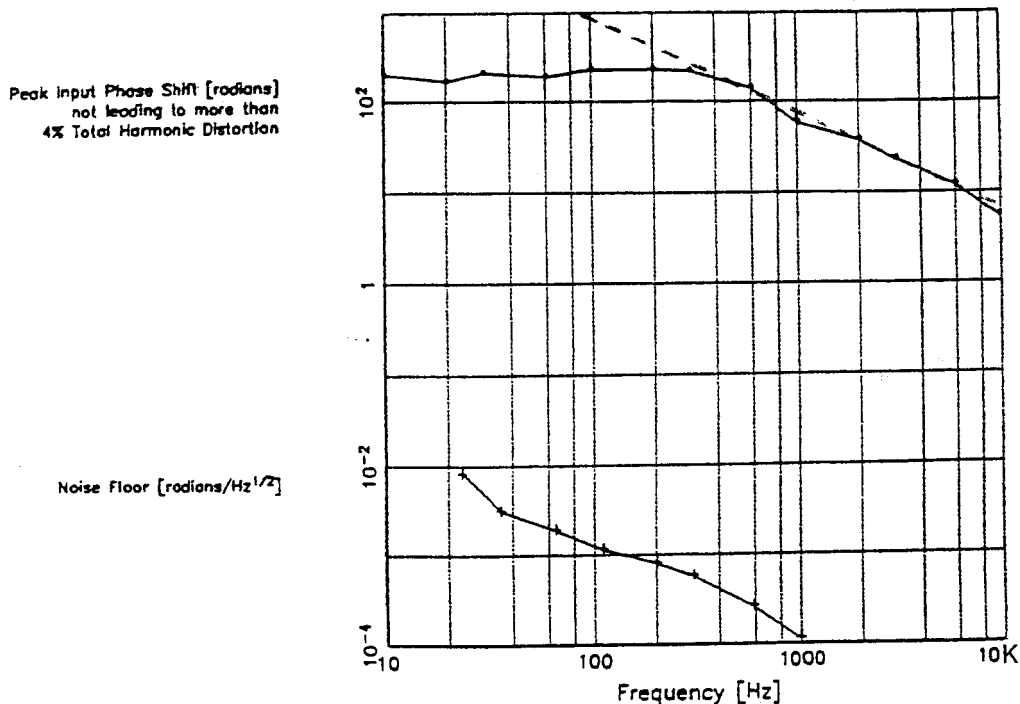


**Figure 5.** Dynamic range of the symmetric demodulator. The dashed line is an extrapolation of the maximum signal, which in this test, was limited to 200 radians due to driving limitations on the piezoelectric cylinders and the amount of attached optical fiber.

### 5. Implementation

The initial performance of the symmetric demodulator has been extremely promising. However, implementation of demodulator does have some restrictions. First, the demodulator scheme requires a 3x3 coupler in the sensor versus a 2x2 coupler, and hence, the minimum number of fibers needed to operate the fiber optic sensor is four (one input and three outputs for the Mach-Zehnder interferometric configuration). Implementation of the symmetric demodulator with a Michelson interferometer (having a single coupler with mirrored fiber end) is not readily accomplished and would require a "tap" coupler so that one of the three output fibers could also serve as the input fiber supplying the coherent light as illustrated in Figure 6. Thus, for systems where channel reduction is paramount, the improved performance and cost of a 3x3 based demodulation system may not be warranted over that of a 2x2 based phase generated carrier implementation.

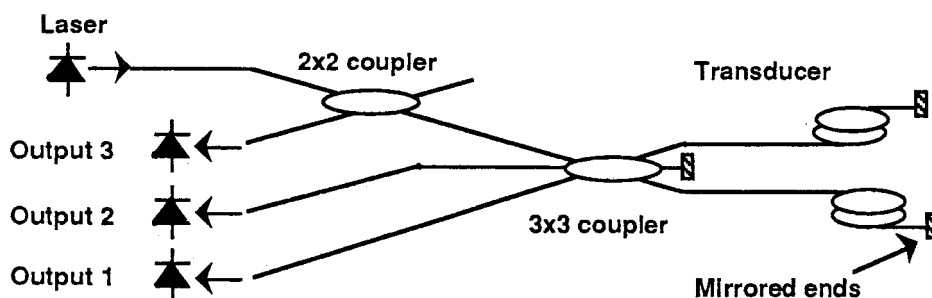


**Figure 6.** A Michelson interferometer using a 3x3 coupler and a 2x2 "tap" coupler to acquire the third output of the sensor.

## 6. Acknowledgements

This work was supported by the Naval Postgraduate School Direct Funded Research Program, the National Oceanic and Atmospheric Administration, and the Naval Sea Systems Command.

## 7. REFERENCES

1. J. A. Bucaro, H. D. Dardy, and E. F. Carome, "Fiber optic hydrophone", *J. Acoust. Soc. Am* **62**, 302 (1977).
2. A. Dandridge, A. B. Tveten, and T. G. Giallorenzi, "Homodyne demodulation scheme for fiber optic sensors using phase generated carrier", *IEEE J. Quantum Electron.* **QE-18**, 1647 (1982).
3. K. P. Koo, A. B. Tveten, and A. Dandridge, "Passive Stabilization Scheme for Fiber Interferometry Using (3 x 3) Fiber Directional Couplers", *Appl. Phys. Lett.* **41**, 616 (1982).
4. M. A. Davis, A. D. Kersey, M. J. Marrone, and A. Dandridge, "Characterization of 3 x 3 Fiber Couplers for Passive Homodyne Systems: Polarization and Temperature Sensitivity", paper WQ2, *Proc. Optical Fiber Communications Conference*, Houston, TX, Feb. 6-9, 1989.
5. D. L. Gardner and S. L. Garrett, "Fiber optic seismic sensor", *Fiber Optic and Laser Sensors V*, *Proc. Soc. Photo Optical Inst. Eng. (SPIE)* **838**, 271-278 (1987); "Multiple axis fiber optic interferometric seismic sensor", U. S. Pat. No. 4,893,930 (Jan. 16, 1990).
6. D. A. Brown, T. Hofler, and S. L. Garrett, "High sensitivity, fiber-optic, flexural disk, hydrophone with reduced acceleration response", *Fiber and Int. Optics*, **8**(3), pp. 161-191, (1989); U. S. Pat. No. 4,959,539 (Sept. 25, 1990).
7. S. L. Garrett, D. A. Brown, B. L. Beaton, K. Wetterskog, and J. Serocki, "A general purpose fiber-optic interferometric hydrophone made of castable epoxy", *Fiber Optic and Laser Sensors VIII*, *Proc. Soc. Photo Optical Inst. Eng. (SPIE)* **1367**, 13-29 (1990).
8. D. A. Brown, S. L. Garrett and D. A. Danielson, "Fiber-optic ellipsoidal flextensional hydrophones", in *Fiber Optic and Laser Sensors VII*, *Proc. Soc. Photo-optical Inst. Eng. (SPIE)*, **1169**, pp. 240-248, (1989); U. S. Pat. No. 4,951,271 (Aug. 21, 1990).
9. D. A. Brown, "Optical fiber interferometric acoustic sensors using ellipsoidal sell transducers", Ph. D. Dissertation, Engineering Acoustics, Naval Postgraduate School, Monterey, CA, June, 1991.
10. C. B. Cameron, R. M. Keolian, and S. L. Garrett, "A Symmetric Analogue Demodulator for Optical Fiber Interferometric Sensors", *Proc. 34th Midwest Symposium on Circuits and Systems (IEEE)*, Monterey, CA, May 14-17, 1991.
11. C. B. Cameron, "Recovering Signals from Optical Fiber Interferometric Sensors", Ph. D. Dissertation, Electrical Engineering, Naval Postgraduate School, Monterey, CA, June, 1991.